Blast- Induced Structural and Crack Response of a Brick Residential Structure Near an Aggregate Quarry

By

Catherine Aimone-Martin and Charles H Dowding

Abstract and Introduction

This article summarizes an investigation of the structural response of a brick façade home in New Mexico. The subject Ricter residence was located some 1100 to 1400 ft away from an aggregate quarry, and was subjected to a maximum peak particle velocity and air blast over pressure of 0.29 ips and 122 dB, respectively. Superstructure (corner) and mid-wall responses to blasting and human induced activities were measured. An existing exterior crack in the brick work was instrumented to measure crack width response to blasting, human induced activities, and environmentally induced changes in temperature and humidity. Crack and structure response data were correlated with ground velocity and airblast excitations. Amplification of ground motions at the upper structure were calculated and compared with values for typical wood frame structures. The natural frequency and damping characteristics of the structure were determined to compare with measured amplification values. Wall strains produced by bending and in-plane tension strains were computed from upper corner structure response and compared to failure strains for drywall and brick veneer. Calculated strains were found to be far lower than those required to crack brick and environmentally induced crack response was found to be far greater than that caused by blast induced ground motion or airblast overpressures.

---

1) Professor of Mineral and Geological Engineering, New Mexico Institute of Technology, Socorro, New Mexico, USA
2) Professor of Civil and Environmental Engineering, Northwestern University, Evanston, Illinois, USA

Vibration and Airblast Instrumentation to Measure Structural Response

Figure 1 shows a plan view of the instrumentation locations within, and exterior to, the Ricter residence. The location of the interior, single component velocity transducers placed in the upper (S2) corner, lower (S1) corner, and at the mid-wall in the northeast bedroom are indicated. LARCOR™ multi-component seismographs were used to digitally record four channels of seismic data. The exterior (master) unit (S/N 2279) consisted of a triaxial geophone and an airblast microphone. The triaxial geophone was buried at a depth of 6 in., and oriented so that the radial, R, component was directed toward the north and parallel with one of the axes of the house. This orientation is based upon recording motions that are parallel to one of the house's translation axes rather than the traditional direction relative to the vibration vibration source. The airblast microphone was installed at a height of 18 in. above the ground surface and was used to record the pressure pulses transmitted through the air during blasting.

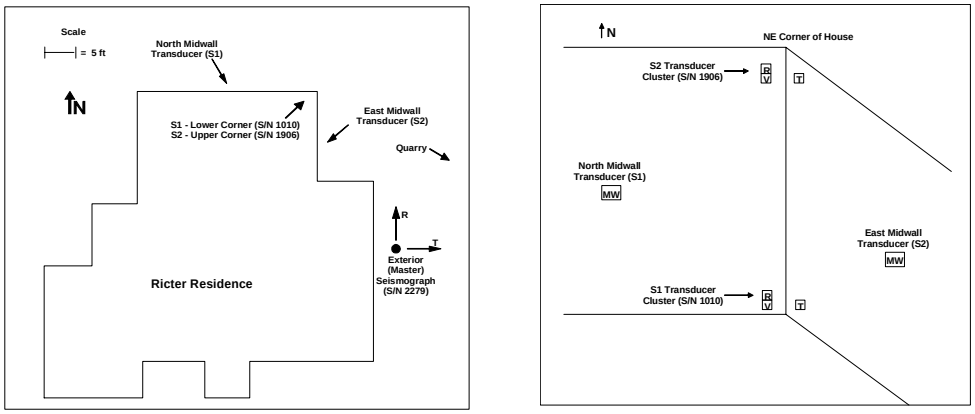

Figure 1: Plan View of Instrumented House (left) and Locations of Velocity Transducers to Measure Structural Response

Both the S1 and S2 seismographs (S/N 1010 and 1906 respectively) were connected to clusters of three single axis transducers in the northeast bedroom corner and one at a mid-wall (north or east wall) as shown in Figure 1 (left). These transducers were affixed to the walls using hot glue to minimize damage during removal. The three corner transducers, labeled R, T, and V in Figure 1 (right), measured whole structure motions in the horizontally radial (north-south), transverse (east-west) , and vertical directions, respectively. The mid-wall transducers measured horizontal motions during wall flexure or bending. Photographs of all transducer locations are shown in Figure 2.

Figure 2 Photographs of Transducer Locations for Measurement of Structural Response Showing Individual Midwall transducers (left and right) as well as corner clusters (top and Bottom)

The three seismographs used were connected in series, with the exterior as the master unit, and the interior as slave units. The master unit was set in the trigger mode. As such, the unit activated automatically when it detected a ground velocity or airblast greater than the pre-set trigger levels. Upon triggering, the master unit delivered a 1 volt pulse to the slave units via the serial cable. The slave units, set in the manual mode, activated and began recording data upon receiving the 1 volt pulse. The master and slave units recorded with a common time base. Thus, the seismograph records are time-

correlated, which is critical for later analysis of structural and crack response. Master and slave seismographs each had a range of available settings for recording data. These settings include: 1) trigger levels for the master unit set to 0.03 in. per second (ips) for ground velocity, and 132 decibels (dB) for airblast, 2) sampling rate of 512 samples per second, 3) sampling duration of 7 seconds.

Crack Response Instrumentation

To measure the effect of blasting and climate conditions (temperature and humidity) on changes in the width of an existing exterior crack, Kaman™ eddy-current gages were installed as shown in Figure 3. Each Kaman gage consisted of mounting brackets, an active element, and a target plate. The gage mounting brackets were affixed to the brick exterior of the structure using epoxy to ensure that the brackets remained in rigid contact with the wall. One Kaman gage was installed over an existing crack (crack gage) and another was positioned on the un-cracked brick façade (null gage). The crack gage was installed with each mounting bracket placed on either side of the crack. One bracket held the active element against the target plate (second bracket) at a sufficient gap distance to allow the gage to function properly.

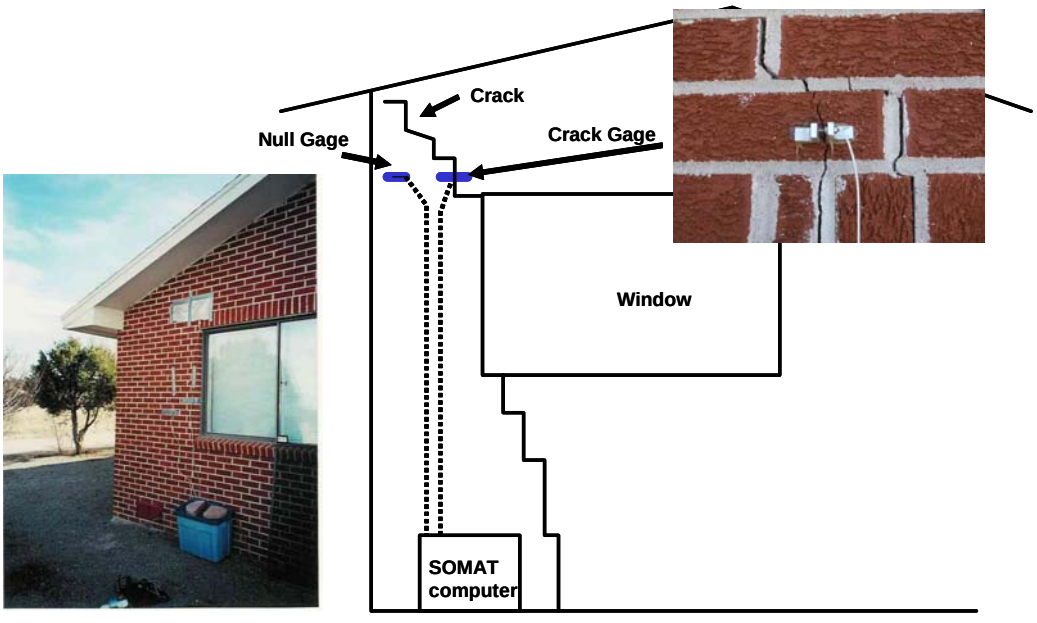

Figure 3: Location of Crack and Null Sensors at the north east Corner of the Structure

Operation of Eddy-current gages relies on the property of electrical induction. The sensor consists of a coil of wire driven by a high frequency current. This current generates a magnetic field around the coil. If a non-magnetic conductive target material is introduced into the coil field, eddy-currents are induced in the surface of the target material. These currents generate a secondary magnetic field in the target, inducing a secondary voltage in the sensor coil (active element), resulting in a decrease in the inductive reactance in the coil. This type of system is also known as variable impedance because of the significance of the impedance variations in defining its complex nature (Hitz and Welsby, 1997).

Ground Motion and Airblast Environment

As shown in Table 1, the blasting and resulting ground motion environment were typical of that found near most quarry operations. Maximum charge weights per 8 millisecond delay varied betwen 116 and 209 lbs. Given the distances between the shot and the Ricter residence shown in Table 1, the range of scaled distances (SD) were 80 to 190 ft./lb.$^{1/2}$. Horizontal ground peak particle velocities (PPV) recorded at the Ricter residence ranged from 0.06 inches per second (ips) to 0.29 ips, while vertical velocities ranged from 0.03 ips to 0.13 ips. Dominant excitation frequencies as calculated by Fast Fourier Transform (FFT) varied between 7.3 Hz and 24.4 Hz. PPV's are well below the generally accepted threshold of cosmetic hairline cracks of 0.5 ips to 0.75 ips for excitation frequencies below 10 Hz. Airblast overpressures recorded at the Ricter residence ranged from 106 to 120 dB.

Shot Date	Time	Distance	Charge Weight/Delay	Scaled Distance	Scaled Distance	GROUND MOTION AND AIRBLAST				
						Peak Particle Velocity	component	Peak Frequency	FFT Frequency	Airblast
		(ft)	(lb)	(ft/lb$^{1/2}$)	(ft/lb$^{1/3}$)	(in/sec)		(Hz)	(Hz)	(dB)
2/17/2003	10:45	1200	178.3	89.9	213.6	0.185	T	19.6	24.4	120
2/26/2003	10:13	1132	186.8	82.8	198.4	0.210	T	12.1	8.4	114
3/3/2002	10:51	1200	116.2	111.3	246.3	0.135	T	13.4	8.3	117
3/5/2003	11:43	1200	175.2	90.7	214.8	0.133	R	12.1	8.5	118
3/6/2003	11:50	1221	203.1	85.7	208.1	0.128	R	8.0	7.3	112
3/7/2003	12:25	1200	118.1	110.4	245.0	0.125	R	9.4	9.5	112
3/12/2003	11:46	1177	136.3	100.8	229.1	0.288	T	11.6	12.8	112
3/13/2003	10:21	1388	137.3	118.5	269.5	0.210	R	9.1	10.0	116
3/25/2003	13:43	1399	138.3	119.0	271.0	0.200	R	9.4	8.3	116
3/28/2003	12:32	1321	201.0	93.2	225.9	0.093	T	10.2	9.4	117
4/1/2003	11:40	1151	208.7	79.7	194.4	0.205	R	9.4	9.1	116
4/4/2003	12:30	1384	172.0	105.5	249.3	0.095	R	8.5	9.3	106
4/8/2003	12:15	1150	151	93.6	216.3	0.290	R	9.1	6.6	112
4/16/2003	10:20	1100	161.6	86.5	202.3	0.108	R	8.0	10.1	114
4/23/2003	10:27	1240	157	99.0	230.2	0.110	R	9.4	8.0	121
4/24/2003	10:30	1200	157	95.8	222.8	0.105	T	11.6	8.0	110
4/29/2003	11:40	1100	138.5	93.5	213.0	0.138	R	9.4	10.5	110
4/30/2003	10:27	1044	181.1	77.6	184.8	0.228	T	14.2	8.3	122

Table 1 Ground Motion and Airblast Environment

Time histories of excitation and measured responses are shown in Figure 4 for the 30 April 2003 event. The upper three time histories are the excitation ground motions and air overpressure. The bottom three time histories are the upper structural response and the crack response.

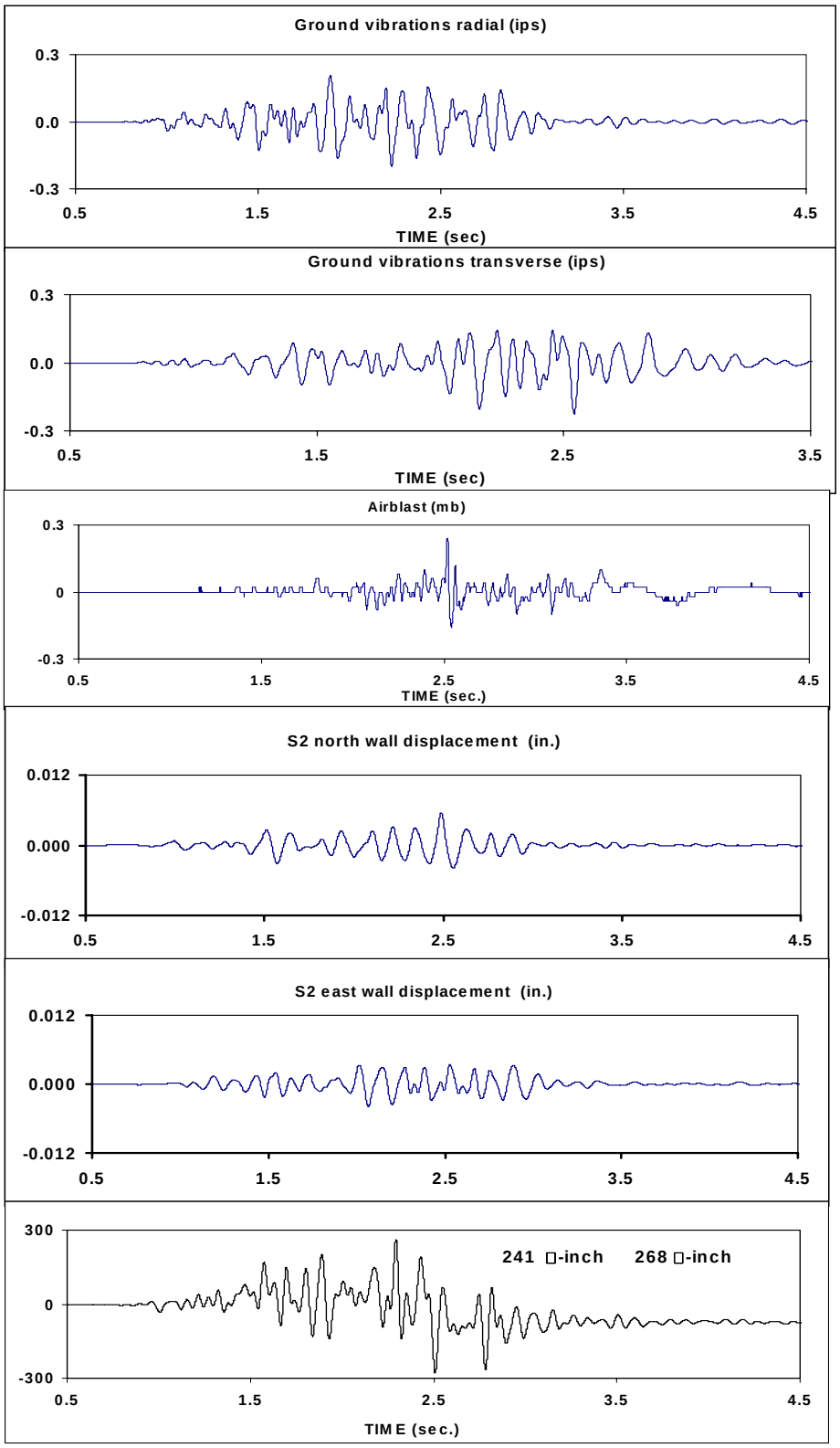

Figure 4: Time Histories of the Excitation (upper three) and Response Motions and Pressures, Response Motions (4 an 5 from top) and Crack Response (bottom)

Structural Response

Peak upper corner responses are compared to the excitation in Figure 4 to the excitation PPV ground motions and air blast overpressures. Responses of north and east walls (radial and tangential directions defined in Figure 1) are compared with the appropriate excitation PPV component. For this structure and range of excitation frequencies it the PPV in the direction parallel to the transducer appears to be a predictor of structural response. Airblast overpressure appears to correlate less well for this structure. This diminished correlation may result from many factors, one of which may be the greater weight of a brick walled structure.

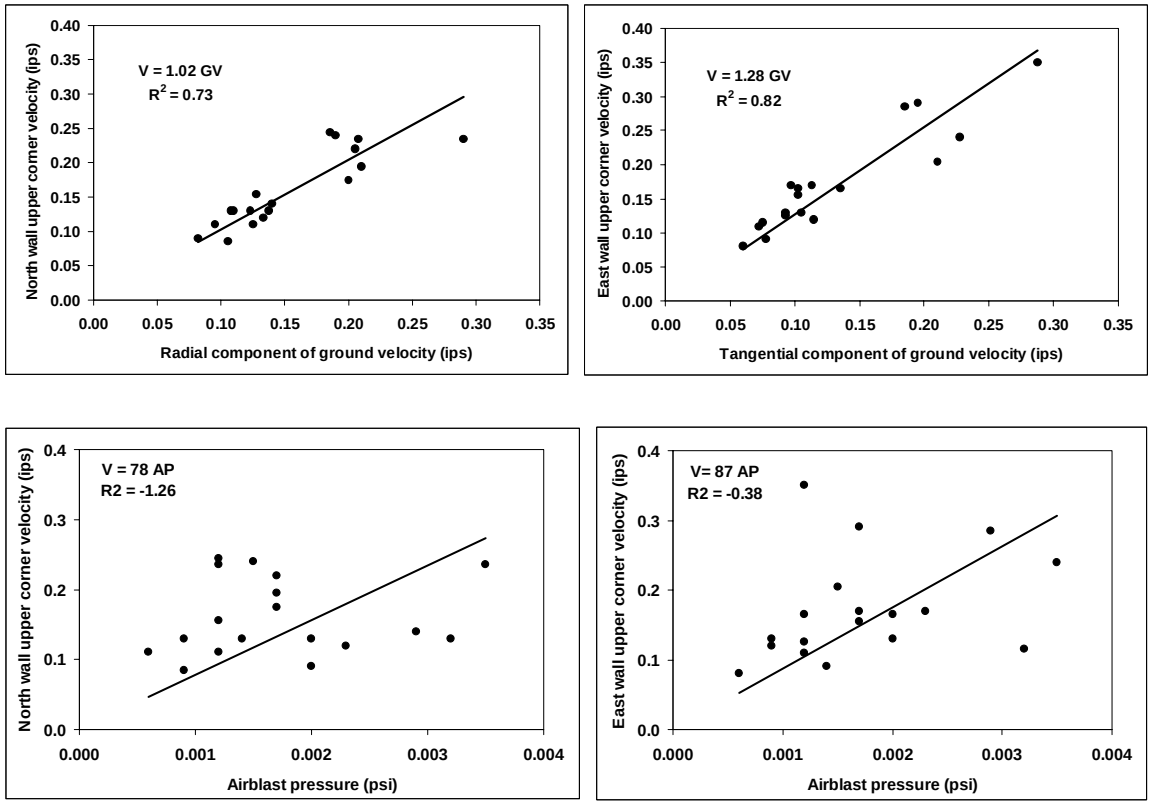

Figure 5: Correlations of Upper Structural Responses with Parallel Directed PPV's and Airblast Overpressures.

Upper Structure Amplification of Ground Velocities

Amplification is a comparative measure of the maximum structure response to ground vibration at the same point in time and can be determined in terms of velocity or displacement. It is similar to the term "dynamic amplification factor" used by seismologists to describe the effects of earthquakes on structures.

Amplification occurs when motion at S2 becomes larger than the motion at S1 and GV. Amplification factor (AF) was defined for blasting vibrations by the U.S.

Bureau of Mines (Siskind, et al., 1980) as the ratio of the peak upper structure velocity ($S2_{peak}$) divided by the preceding ground velocity (GV) of the same phase, positive or negative, that most likely drive the structure. Figure 4 shows the relationship between predominant frequency (FFT) of the ground velocity and the calculated amplification factors. The maximum structure amplification falls in the range of 8 to 9 Hz. This frequency range corresponds to calculated natural frequencies of the super structure ranging from 8 to 11.8 Hz. Structures typically exhibit maximum amplification when vibrated at their natural frequency.

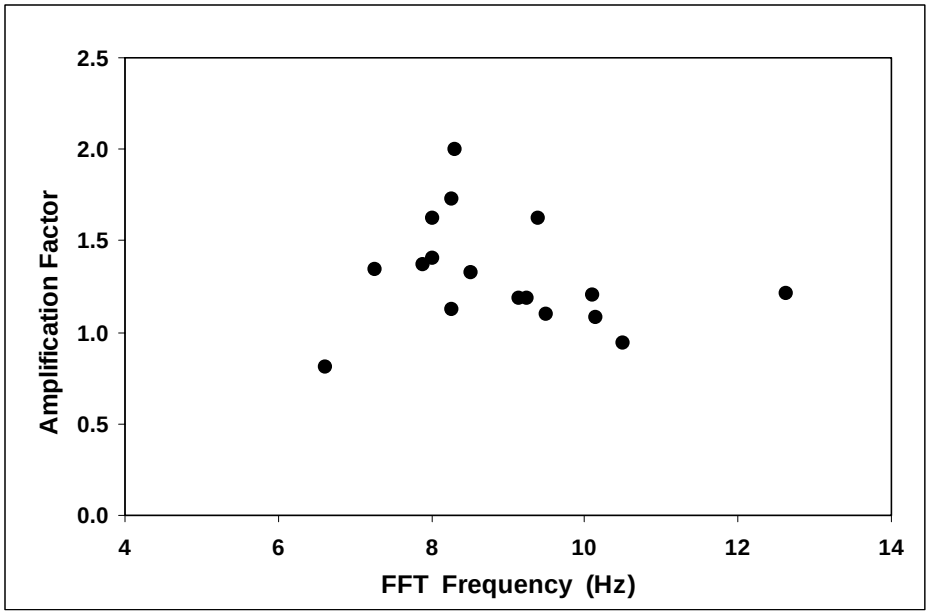

Figure 6: Comparison of Amplification Factor and Dominant Excitation Frequency Showing Greater Amplification between 8-9 Hz, the Natural Frequency of the Sturcture.

Strains

The magnitude of induced strains in structure components determines the likelihood of cosmetic cracking in residences. Global shear strains may be estimated from differential structure motions calculated from the difference in displacements at the upper, S2, and lower, S1, in direction parallel to the plane of the wall of interest. Velocity time histories at S1 and S2 are first integrated to obtain displacement time histories, then the largest time correlated difference between corner responses (S2 minus S1) is found. Plots of the differential and component displacements time histories for the April 30 event is shown in Figure 7

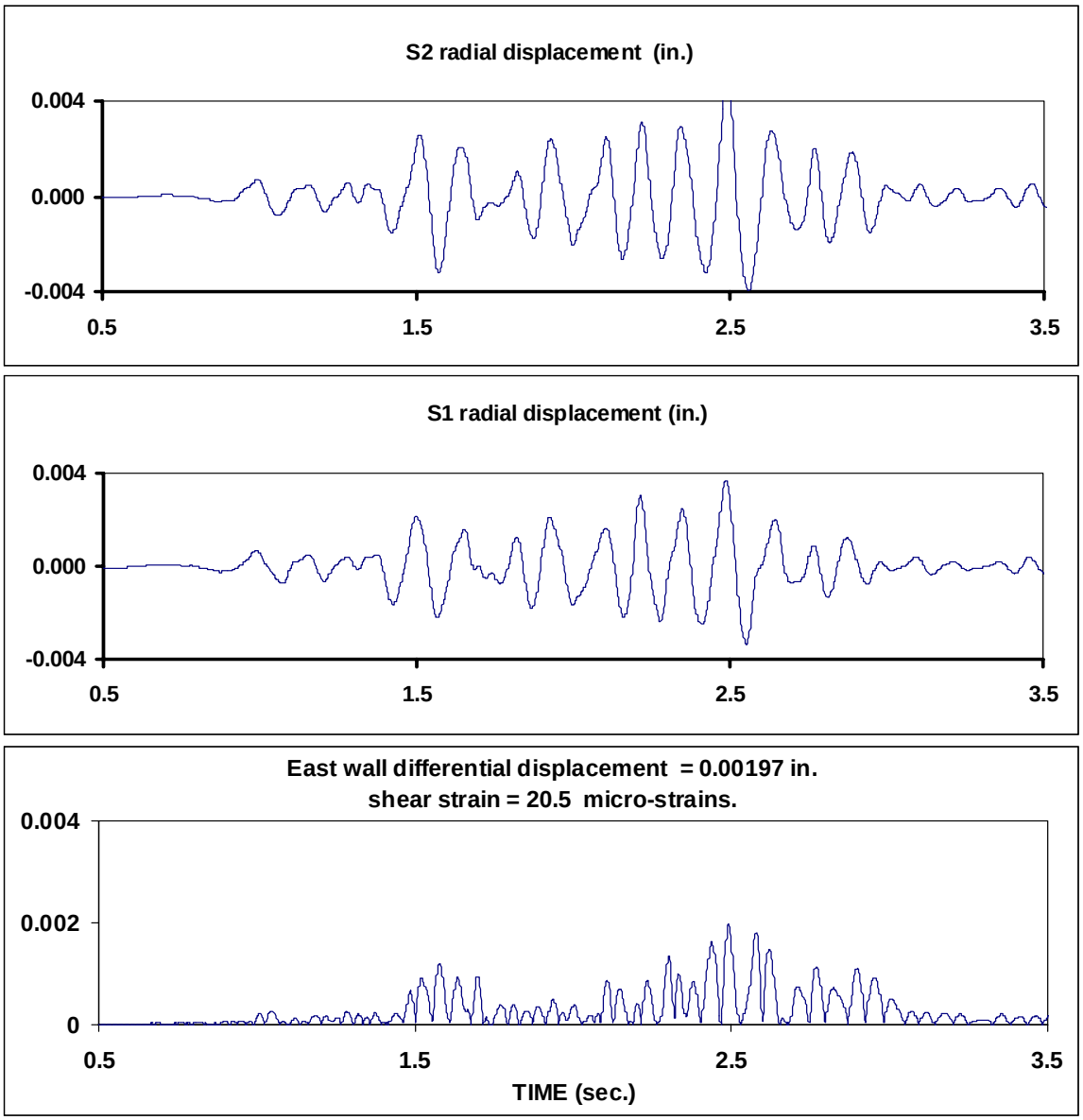

Figure 7: Displacement Time Histories (Integrated Velocity Time Histories) of the Upper Corner in the Transverse Direction and the Resulting Absolute Value of the Difference between the Upper and Lower Displacements (δ_{max}) from which Strain is Calculated.

Global shear strain is determined by the following:

$$\gamma_{max} = \left(\frac{\delta_{max}}{L} \right)$$

where

γ_{max} = global shear strain (micro-strains or 10^{-6})

δ_{max} = maximum differential displacement, S2 – S1 (in.)
L = height of the wall subjected to strain (in.)

In-plane tensile strain, $\varepsilon_{Lmax,}$ is calculated from global shear strain by the equation:

$$\varepsilon_{L\,max} = \gamma_{max}(\sin\theta)(\cos\theta)$$

where θ is the interior angle of the longest diagonal of the wall subjected to strain with reference to a horizontal. Theta, θ, is calculated by taking the inverse tangent of the ratio of wall height to wall length.

Walls of structures, which approximate flexible plates, tend to flex in a direction perpendicular to the plane of the wall with maximum displacements in the first mode of response at the middle of the wall. Such wall flexure is directly related to the bending strain induced in the walls and can be modeled as a beam fixed at both ends, at the foundation (S1) and at the roof (S2). It has been determined that the foundation is well coupled to the ground, or "fixed". However, the roof can be modeled with varying degrees of "fixity", ranging from relatively unconstrained to highly fixed. Bending strain is most conservatively estimated with the fixed-fixed analogy because this model predicts the highest strains in walls per unit of maximum relative displacement. These out of bending strains can be calculated as:

$$\varepsilon = \left(\frac{d 6 \delta_{max}}{L^2} \right)$$

where

ε = bending strain in walls (micro-strains or 10^{-6})
d = the distance from the neutral axis to the wall surface, or one half the thickness of the wall subjected to strain (in.)

For the Ricter residence, the transverse component of the GV excitation induces "out of plane" strain in the east wall of the structure, while the radial component of GV induces "out of plane" strain in the north wall.

Table 2 is a summary of the maximum calculated strains induced by ground motion excitation for the Ricter residence. The maximum recorded whole structure differential displacement was 0.0093 in. The maximum and minimum global shear strains calculated were 47 and 3 micro-strains respectively. The maximum in-plane tensile strain calculated was 21 micro-strains. According to Dowding (1985), the range of failure in the gypsum core of drywall is 300 to 500 micro-strains. Using the maximum observed tensile strain of 21, the factors of safety against cracking were 14 to 24 for the interior drywall and well above the safe limits of cracking. The induced strains in the drywall never exceeded the elastic limit of the material and no permanent deformation could have occurred. Maximum bending strains computed for mid-wall flexure during the ground vibration phase of structure motions were 11 and 10 micro-strains for the east and

north walls, respectively. Therefore, any cracks in interior drywall cannot be attributed to blasting strains.

Shot Date	Maximum differential wall displacement, □S (in.)		Maximum shear strain (□-strain)		Maximum in-plane tensile strain (□-strain)		Maximum bending strain in the ground motion phase (□-strain)		Maximum ground velocity (ips)	
	east wall	north wall	east wall	north wall	east wall	north wall	east wall	north wall	Radial	Transverse
2/17/2003	0.00120	0.00151	15.73	12.50	7.02	5.58	TF	4.88	0.140	0.185
2/26/2003	0.0013	0.0022	23.13	13.54	10.32	6.04	11.02	6.02	0.190	0.210
3/3/2002	0.0011	0.0093	11.46	9.69	5.12	4.33	7.89	3.93	0.123	0.135
3/5/2003	0.00092	0.00089	9.57	9.27	4.27	4.14	8.69	4.56	0.133	0.113
3/6/2003	0.0008	0.0008	8.54	8.61	3.81	3.85	8.76	7.16	0.128	0.093
3/7/2003	0.0007	0.0007	7.12	7.29	3.18	3.25	6.82	3.25	0.125	0.073
3/12/2003	0.00147	0.00166	17.3	15.3125	7.72	6.84	20.64	9.60	0.185	0.2875
3/13/2003	0.00115	0.0017	17.7083	11.98	7.90	5.35	8.87	7.06	0.21	0.1025
3/25/2003	0.00109	0.00115	11.98	11.35	5.35	5.07	7.08	6.71	0.200	0.098
3/28/2003	0.00054	0.0053	5.63	5.52	2.51	2.46	5.13	3.69	0.210	0.093
4/1/2003	0.0018	0.0016	18.50	16.60	8.26	7.41	18.10	9.70	0.205	0.195
4/4/2003	0.00044	0.00074	7.70	4.60	3.44	2.05	4.40	4.00	0.095	0.060
4/8/2003	0.00114	0.0015	15.60	11.88	6.96	5.30	9.26	10.42	0.290	0.103
4/16/2003	0.00275	0.00448	46.67	28.65	20.83	12.79	5.37	9.42	0.108	0.078
4/23/2003	0.00075	0.00074	7.70	7.80	3.44	3.48	6.40	5.80	0.110	0.075
4/24/2003	0.00072	0.00087	9.06	7.50	4.04	3.35	6.75	2.85	0.105	0.105
4/29/2003	0.00083	0.00105	10.94	8.65	4.88	3.86	6.04	4.35	0.138	0.115
4/30/2003	0.0017	0.00197	20.52	17.71	9.16	7.91	8.17	7.13	0.208	0.228

TF tranducer failure

Table 2: Tablulation of Calculated Strains for All Events

For comparison, the maximum bending strains induced in the north and east mid-wall by airblast pressures were 15.2 and 1.32 micro-strains in the east and north walls. It is not possible that bending strain contributes to wall cracking at these levels of vibrations and airblast. However wall motions produce noise inside structures during wall flexure and thus can be responsible for annoyance.

Long-Term or Environmental and Weather Induced Crack Response

Long- term changes in crack width are presented in Figure 6 along with outside temperature and humidity for a period of 73 days (1800 hours). A portion of the crack data were not recorded, which is reflected in the gap in crack response around 1000 hours. In general, crack movement follows the trend in exterior humidity; when the humidity increases, the crack closes (negative change). The crack also closes with increase in temperature. Normal 24-hour changes in temperature, humidity and crack response are shown in Figure 7 over the last 5.4 days of the study to better show the diurnal cycles. The unusual temperature spike (up to 108 degrees F) in the early morning cannot be explained. The large variation in crack width over a ½ day cycle can be clearly observed. The largest measured change over this daily cycle was some 1500 micro-strains. This daily change far exceeds the largest change in crack width during blasting (268 micro-inch on April 30 shown in Figure 4). Furthermore, the greatest overall change in crack width for the duration of the study was 8530 micro-inch. This weather-induced change in crack width is the largest contributing factor to crack extension and widening over time. Blasting vibration influence on changes in crack widths are negligible compared to the influence of climate. Hence, blasting is unlikely to be the source of brick cracking.

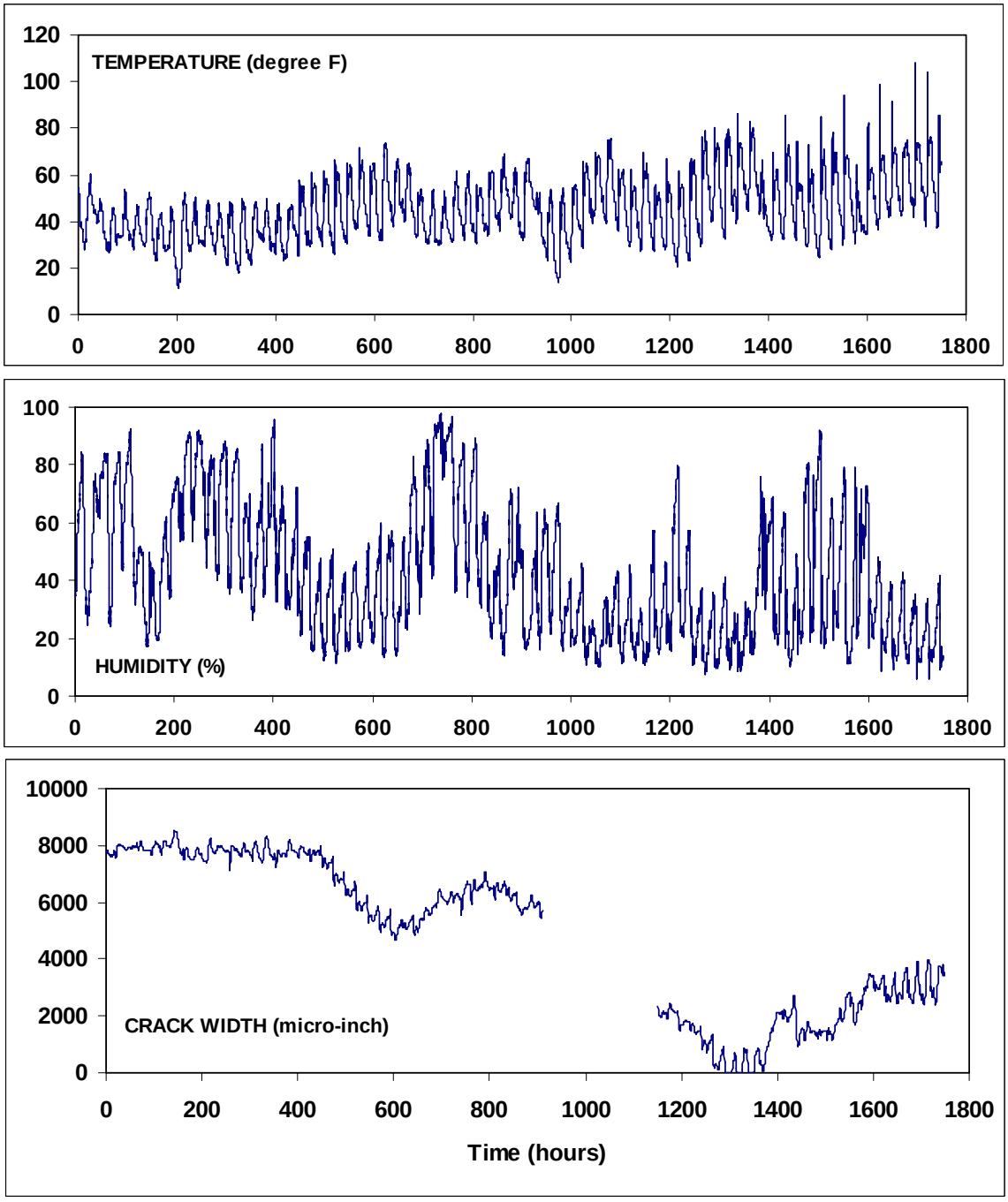

Figure 8: Comparison of Long Term Crack Response with Outside Temperature and Humidity

Crack width responses recorded from the human induced activities ranged between 2.46 to 178.5 micro-inch compared with blast-induced displacements from 83 to 268 micro-inch

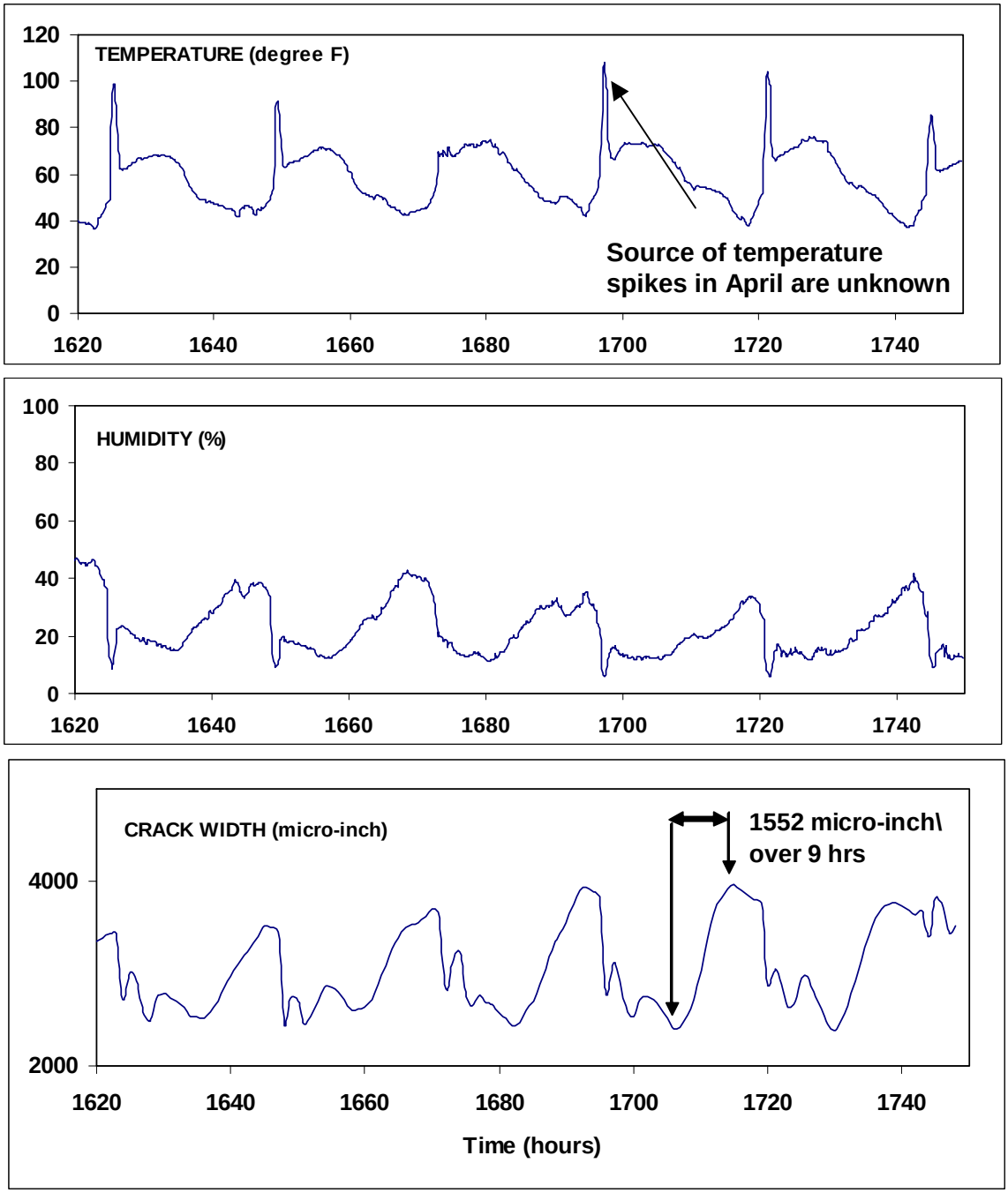

Figure 9: Comparison of Daily Changes in Crack Width with Changes in Outside Temperature and Humidity.

4.0 Conclusions

- Less correlation was found between peak airblast levels and structure response as there was between peak ground motion and structural response; airblast overpressures may not be sufficiently energetic to induce consistent upper structure and mid-wall motions in the brick faced single story structure.

- Calculated natural frequencies of the structure ranged from 8.0 Hz to 12 Hz, with an average of 9.3 Hz. The average calculated damping was 7.0%. Natural frequency and damping were within the ranges for typical residential structures; 4 Hz to 12 Hz (natural frequency) and 2 to 10% (damping).

- Average and peak time correlated amplification of upper structure response with ground motions ranged from 1.06 to 2.33 in terms of velocity and from 1.05 to 2.76 in terms of displacement. The average amplification factor was 1.5. The maximum structure amplification occurred with dominant excitation frequencies of 8 to 9 Hz. Amplification factors were less than average values found in previous research.

- Calculated maximum in-plane tensile wall strain from ground motion excitations was 21 micro-strains. Calculated maximum mid-wall bending strain was also 21 micro-strains. Maximum airblast induced mid-wall bending strains were 15 micro-strains. These blast-induced strains are far less than the 700 to 1000 micro-strains to fail brick..

- The maximum recorded crack width response from blasting was 268 micro-inches, while temperature and humidity changes over the 73 day study period produced a maximum crack response value of 8530 micro-inches. The largest ½ day temperature cycle induced change in crack width was 1552 micro-inches. Therefore, blasting vibration influence on change in crack width is negligible compared with the influence of environmental/weather or temperature changes.

ACKNOWLEDGEMENTS

This project was sponsored and supported by Lafarge Southwest, Inc. with the generous cooperation of Leon and Diane Ricter. The authors acknowledge the guidance and contributions of Lafarge employees Teresa Conner and Ken Ford. Lee Buckley, of Buckley Powder Co., was instrumental in providing blasting data and participating on this project. The following undergraduates and graduate students at the New Mexico Institute of Mining & Technology assisted with the instrumentation, made the calculations and wrote large sections of the report: Rachel Ehlers, Barrett Friesen, Keli Goulart, Duncan Langlois, Jessica Rollings, Tomas Villegas. This project provided field experience for students participating in the course ME 545, Advanced Vibration Control and Analysis. Large sections and all of the tables and figures of this article were directly extracted from the project report. Crack monitoring instrumentation and technical assistance were provided by the Infrastructure Technology Institute at Northwestern University through its program to commercialize new instrumentation to assist construction of the transportation infrastructure.

REFERNCES

Aimone-Martin, C.T., M.A. Martell, L.M. McKenna, D.E. Siskind, and C.H. Dowding, 2003, Comparative Study of Structure Response to Coal Mine Blasting, prepared for the Office of Surface Mining Reclamation and Enforcement, Pittsburgh.

Aimone-Martin, C.T. and K. Eltschlager, 2003. Guidelines for Measuring and Evaluating Residential Structure Response, for the Office of Surface Mining and Reclamation Enforcement, Aimone-Martin Associates, LLC.

Dowding, C.H., 19856, Blast Vibration Monitoring and control, Prentiss-Hall

Hitz, T. and S.D. Welsby, 1997, True Position Measurement with Eddy-Current Technology, Sensors Magazine, pp. 13.

McKenna, L., 2002, Velocity Response of Atypical Residential Structure and Autonomous Crack Monitoring, M.S. Thesis , Northwestern University.

Mercer, M., 2003, Data Filter Software, M.S. Thesis, New Mexico Institute of Mining and Technology.